Millimeter-wave Aperture Synthesis Imaging of Vega: Evidence for a Ring Arc at 95 AU

D.W. Koerner[1], A.I. Sargent[2], and N.A. Ostroff[1]

ABSTRACT

We present the first millimeter-wave aperture synthesis map of dust around a main sequence star. A 3″ resolution image of 1.3 mm continuum emission from Vega reveals a clump of emission 12″ from the star at PA 45°, consistent with the location of maximum 850 μm emission in a lower resolution JCMT/SCUBA map. The flux density is 4.0±0.9 mJy. Adjacent 1.3 mm peaks with flux densities 3.4±1.0 mJy and 2.8±0.9 mJy are located 14″ and 13″ from the star at PA 67° and 18°, respectively. An arc-like bridge connects the two strongest peaks. There is an additional 2.4 ±0.8 mJy peak to the SW 11″ from the star at PA 215° and a marginal detection, 1.4±0.5 mJy, at the stellar position, consistent with photospheric emission. An extrapolation from the 850 μm flux, assuming $F_{1.3mm-0.85mm} \propto \lambda^{-2.8}$, agrees well with the total detected flux for Vega at 1.3 mm, and implies a dust emissivity index, β, of 0.8 We conclude that we have detected all but a very small fraction of the dust imaged by SCUBA in our aperture synthesis map and that these grains are largely confined to segments of a ring of radius 95 AU.

1. Introduction

The IRAS detection of excess infrared emission from Vega (α Lyrae) heralded the discovery that dust grains surround many nearby stars (Aumann et al. 1984; Gillett 1986). High-resolution images at wavelengths ranging from the optical to millimeter regimes have since revealed that, in many cases, the dust around similar "Vega-excess" stars is configured in circumstellar disks and rings (Smith & Terrile 1984; see Koerner 2001 for a review). Some of the more massive disks surround stars with ages of order 10 Myr (e.g., Smith & Terrile

---

[1]University of Pennsylvania, David Rittenhouse Laboratory, 209 S. 33rd St., Philadelphia, PA 19104-6396

[2]Division of Physics Mathematics and Astronomy, California Institute of Technology, Pasadena, CA 91125

1984; Jura 1991; Zuckerman & Becklin 1993a) and are readily explainable as the end stages of protostellar/protoplanetary disks like those around younger T Tauri stars (e.g., Beckwith & Sargent 1993). The persistence of material in orbit around older stars like Vega (age ∼350 Myr; Maeder & Meynet 1988) is more problematic, since radiation pressure and Poynting-Robertson drag should have dispersed any grains on much shorter timescales. Traditionally, this conundrum has been resolved by postulating an unseen population of asteroidal or cometary bodies that collisionally regenerate a "debris disk" (e.g., Backman & Paresce 1993), although particles may also be dynamically trapped in mean motion resonances with larger orbiting bodies (Ozernoy et al. 2000).

Coronagraphic imaging of β Pic quickly provided a clear picture of its circumstellar disk (Smith & Terrile 1984). However, it has proved difficult to establish unambiguously the distribution of dust around Vega. The first IRAS observations resolved the 60 μm emission in a 25″ beam and indicated a 60-100 μm color temperature of 85 K (Aumann et al. 1984). Gillett (1986) estimated a size of 29″ × 25″ (FWHM) at PA 85° and postulated the presence of a dust reservoir radially confined between 36 and 170 AU for large grains ($> 100\mu$m), or between 14 and 400 AU for small grains ($< 10\mu$m). He also noted that grains smaller than 1.1 mm should have been depleted by Poynting-Robertson drag. A re-examination of the original resolved 60 μm emission led to a source size of 27″ × 27″ (FWHM), implying a radius of 106 AU and grains ranging in size from 0.1 to 10 μm (van der Bliek et al. 1994). A pole-on configuration was inferred from the circular symmetry and is consistent with the stellar orientation implied by optical spectroscopy (Gulliver et al. 1994). Kuiper Airborne Observatory (KAO) measurements by Harvey et al. (1984), in 30″ and 43″ beams at $\lambda = 47$ and 95 μm, yielded a lower color temperature, 78 K, than IRAS, and suggested that different amounts of material are enclosed by the different beams. Combining these results with measurements in KAO apertures placed 1′ away from the star, these authors proposed that the extent of the dust around Vega was as large as 46″(FWHM). Recent ISOCAM observations at 60 and 90 μm support this suggestion, yielding Gaussian widths (60% peak value) of 22″ ± 2″ and 36″ ± 3″, respectively (Heinrichsen et al. 1998). Deconvolution of the 60 μm ISOCAM image was found to be consistent with an extended source surrounded by a ring of 42″ diameter. ISOPHOT measurements from 25 to 200 μm imply a color temperature of 73 K, a grain emissivity index, $\beta = 1.1$, where emissivity $Q \propto \lambda^{-\beta}$, and the presence of grains of size 110 μm (Heinrichsen et al. 1998).

Initial observations of Vega at sub-millimeter wavelengths were carried out using beams of diverse sizes which complicated interpretation (Chini et al. 1990; 1991; see discussion in Zuckerman & Becklin 1993b). A seven-point map at $\lambda = 800\mu$m, extending to 16″ from the star, revealed excess emission in an 18″ diameter field 8″ E and 14″ N of the stellar position (Zuckerman & Becklin 1993b). This first indication of asymmetric morphology also demon-

strated that the source extended beyond many of the beams used in early submillimeter-wave measurements.

The asymmetric distribution of dust was dramatically confirmed by Holland et al. (1998) (hereafter HGZWM) in their 850 μm image of Vega obtained at the JCMT using the SCUBA bolometer array. Although extended emission appears circular at the lowest intensity levels in this image, a more linear core oriented at PA $\sim$45° encompasses a bright peak at 9″ (70 AU) from the estimated position of the star. Combining the SCUBA results with Vega fluxes from 10μm to 1 mm, Dent et al. (2000) (hereafter, DWHG) find a dust temperature of 80 K, effective grain sizes of 70 μm, and $\beta = 0.8$. Their modelling suggests that the dust is confined to a ring centered on the star with inner radius > 80 AU and outer radius < 120 AU (i.e., between 10″ and 15″ from the star). The brightness asymmetry seen in the SCUBA maps demands density enhancements of at least a factor of 2 in the NE sector of the putative ring. With the higher resolution attainable with the Owens Valley Radio Observatory (OVRO) millimeter-wave array, we can image the distribution of dust grains around Vega in greater detail. Here we present 3″ resolution aperture synthesis images of 1.3 mm emission from Vega that strongly support the pole-on ring hypothesis.

2. Observations and Results

Two low-resolution configurations (baseline lengths from 15 to 115 m) of the six 10.4 m telescopes of the OVRO millimeter array were used to observe Vega in the 1.3 mm band in four 1 GHz bands at 229.0, 230.5, 233.5, and 235.0 GHz. Observations were made on 15 occasions between fall 1999 and spring 2001. These observing cycles each lasted from 4 to 10 hours and included 25 minute integrations on Vega interspersed with 10 minute integrations on 3C345 for phase and amplitude visibility calibration. The flux density for 3C345 was based on measurements of Neptune and Uranus and varied between 4.0 and 4.6 Jy during the course of the project. The phase center of the observations was the optical position of Vega, α(1950) $8^h35^m14.655^s$, δ(1950) $+ 38°44'09.68''$, modified by proper motions $\Delta\alpha$ = 201 mas/yr and $\Delta\delta$ = 285 mas/yr. These proper motions resulted in a total positional shift of less than 0.5″ throughout the observing period. Visibilities were calibrated using Caltech's MMA software and were combined with NRAO's AIPS package. The AIPS task, IMAGR, was used to make a map which combined natural weighting with a Gaussian taper. A taper with half-power radius of 80 kλ yielded the best signal to noise ratio. The resulting synthesized beam size is 3.3″ × 2.9″ (FWHM) at PA 119° and the rms noise amplitude is 0.5 mJy.

Continuum emission is detected at several locations in the 1.3 mm image of Vega dis-

played in Fig. 1a. For each, the separation from the star and flux density is listed in columns 1-3 of Table 1. The brightest peak lies $12.2'' \pm 0.6''$ NE of the stellar position (95 AU at the 7.8 pc distance of Vega) and is flanked by two fainter detections. The brighter of these is linked to the main peak by an arc of low-intensity emission. The location of the 1.3 mm maximum is consistent with that of the peak of 850 μm emission in a $14''$ beam found by HGZWM, $9'' \pm 2''$ NE of the star. An additional weaker source is seen SW of the star at a distance of $11'' \pm 1''$ (86 AU). Its location and brightness relative to the NE intensity enhancements are also consistent with the morphology of the SCUBA map. Our marginal detection of radiation at the stellar position, 1.4 ± 0.5 mJy, is compatible with the expected photopheric value, 2.5 ± 1.0 mJy, extrapolating from model fluxes at shorter wavelengths (Cohen et al. 1992).

Since the emission peaks in our map are not far from the half-power radius of the primary OVRO array beam, $\theta_B/2 = 16''$, their brightness is under-represented in Fig. 1a. Correction for this diminution was carried out with AIPS task PBCOR and produced the map displayed in Fig. 1b. The corresponding flux densities are listed in column 4 of Table 1. For comparison with our image, the 850 μm fluxes (HGZWM) must be extrapolated with an appropriate relation, $F_\lambda \propto \lambda^{-\alpha}$. These extrapolated values are tabulated in Table 1, columns 5 and 6, for $\alpha = 2$ and 3 respectively. Corresponding SCUBA fluxes are listed in Column 7. For $\alpha = 2$, the fluxes listed in column 4 account for only 75% of the 850μm flux; with $\alpha = 3$, the OVRO and SCUBA fluxes agree within the uncertainties.

3. Discussion

The $3''$ resolution OVRO maps in Fig. 1 strongly support the hypothesis that the dust around Vega is distributed in a clumpy ring, as DWHG suggested. Emission appears at distances of 85 to 110 AU from the star. Its brightness and distribution is consistent with the size and asymmetry of the emission in the $14''$-resolution SCUBA map. The brightest 1.3 mm clump, at 95 AU, is connected to a neighboring peak by a low-intensity bridge which forms an arc-like structure centered on the star. Dust is also detected on the opposite side of the star at a nearly equidistant position. All the flux from the SCUBA map is recovered in the 1.3 mm detections, if a plausible emissivity law is adopted. This suggests that there is little broad extended emission. However, our observations do not rule out the presence of material beyond the edge of the OVRO primary beam, $16''$ (125 AU), as suggested by 95 and 90 μm measurements (Harvey et al. 1984; Heinrichsen et al. 1998).

The total flux in the 850 μm map of HGZWM, 45.7 mJy, implies a 1.3 mm flux density equal to that of sources detected in our map, 14 mJy, if the wavelength dependence of the flux

density $F_{0.85-1.3mm} \propto \lambda^{-\alpha}$ has $\alpha = 2.8$. HGZWM report a value of $\alpha = 2.7$ for F_λ between 850 μm and 1350 μm in a single aperture centered on the peak of 850 μm emission. For optically thin dust radiating in the Rayleigh-Jeans regime, our best fit value for α implies a grain emissivity, $Q \propto \lambda^{-\beta}$, with $\beta = 0.8$. The same value was derived by DWHG in modeling of fluxes from 10 to 1000 μm and, together with the radial location of the dust, implies grain sizes between 30 and 200μm.

Taken together, our results are consistent with Vega being surrounded by a ring of highly variable density. From model fitting, both to the image of HGZWM and to long-wavelength fluxes, DWHG predicted a circum-Vega ring with density enhancements of a factor of two in the NE segment. Emission at levels less than half that of even the strongest peak in Fig. 1a would be below our 3σ (1.5 mJy) detection threshold. As a consequence, a continuous dust ring remains unseen, but the arc-like structure of the patchy maxima provide compelling evidence for its presence. The detection of a much weaker, but symmetrically placed, dust continuum peak to the SW adds to this evidence. Morever, in Fig. 1b, after correction for the effects of the primary beam, several clumps are detectable at the 2σ confidence level. All lie along a possible orbital trajectory for ring material.

There is some evidence for clumping of dust in rings in other extra-solar systems. The narrow ring around HR 4796 (Koerner et al. 1998; Schneider et al. 1999) shows strong evidence of asymmetric brightening at one ansa (Telesco et al. 2000). This feature has been explained as the result of eccentricity forcing, either by a stellar companion or by an unseen planet (Wyatt et al. 2000). An 850 μm SCUBA image of ϵ Eridanae shows a still greater degree of azimuthal asymmetry (Greaves et al. 1999). The ring discontinuity presented here is even more pronounced. Images in Fig. 1 present a picture that resembles that discovered by stellar occultations of the planet Neptune; partial "ring arcs" were inferred from the fact that occultations were observed only along preferred trajectories (Hubbard et al. 1986). Subsequent Voyager images revealed that the arcs were actually connected by tenuous ribbons of dust (Smith et al. 1989). Theoretical analyses concluded that the material is azimuthally confined by resonant interactions with Neptune's satellite Galatea (Goldreich et al. 1986; Porco 1991; Hanninen & Porco 1997). The observations presented here suggest that there may be useful parallels to be drawn between the ring-arcs associated with Neptune and the distribution of dust around Vega. Future sub-mm and mm-wave observations, especially with SAO's Sub-Millimeter Array (SMA) and with the Combined Array for Research in Millimeter Astronomy (CARMA), should make it possible to determine Vega's dust structure in even greater detail and infer details of any hidden planetary bodies responsible for the morphology of a ring arc.

4. Acknowledgements

REFERENCES

Aumann, H.H., Gillett, F.C., Beichman, C.A., de Jong, T., Houck, J.R., Low, F.J., Neugebauer, G., Walker, R.G., & Wesselius, P.R. 1984, ApJ, 278, L23.

Backman, D.E., & Paresce, F. 1993, in Protostars & Planets III, ed. E.H. Levy & J.I. Lunine, (Tucson: University of Arizona Press), p. 1253

Beckwith, S.V.W., & Sargent, A. I. 1993, in *Protostars and Planets III*, eds. E.H. Levy & J.I. Lunine (Tucson:University of Arizona Press), p. 521

Cohen, M., Walker, R.G., Barlow, M.J., & Deacon, J.R. 1992, AJ, 104, 1650

Chini, R., Krügel, E., & Kreysa, E. 1990, A&A, 227, L5

Chini, R., Krügel, E., & Kreysa, E. 1990, A&A, 227, L5

Chini, R., Krügel, E., Shustov, B., Tutukov, A., & Kreysa, E. 1991, A&A, 252, 220

Dent, W.R.F., Walker, H.J., Holland, W.S., & Greaves, J.S. 2000, MNRAS, 314, 702 (DWHG)

Gillett, F.C. 1986, in *Light on Dark Matter*, ed. F.P. Israel, (Dordrecht: Reidel), p. 61

Goldreich, P., Tremaine, S., & Borderies, N. 1986, AJ, 92, 490

Greaves, J.S., Holland, W.S., et al. 1998, ApJ, 506, 133

Gulliver, A.F., Hill, G., & Adelman, S.J. 1994, ApJ, 429, L81

Hanninen, J., & Porco, C. 1997, Icarus, 126, 1

Harvey, P.M., Wilking, B.A., & Joy, M. 1984, Nature, 307, 441

Heinrichsen, I., Walker, H.J., & Klaas, U. 1998, MNRAS, 293, L78

Holland, W.S., Greaves, J.S., Zuckerman, B., Webb, R.A., McCarthy, C., Couldon, I.M., Walther, D.M., Dent, W.R.F., Gear, W.K., & Robson, I. 1998, Nature, 382, 788 (HGZWM)

Hubbard, W.B., Brahic, A., Sicardy, B., Elicer, L.-R., Roques, F., & Vilas, F. 1986, Nature, 319, 636

Jura, M. 1991, ApJ, 383, L79

Koerner, D.W. 2001, in *The 4th Teton Summer School Conf.: Galactic Structure, Stars, and the Interstellar Medium,* ed. C. W. Woodward, M. Bicay, & J. M. Schull, (San Francisco: ASP), p. 563

Koerner, D.W., Ressler, M.E., Werner, M.W., & Backman, D.E. 1998, ApJ, 503, L83

Maeder, A., & Meynet, G. 1988, A&AS, 76, 411

Ozernoy, L.M., Gorkavyi, N.N., Mather, J.C., Taidakove, & T.A. 2000, ApJ, 537, L147

Porco, C.C. 1991, Science, 253, 995

Schneider, G., Smith, B.A., Becklin, E.E., Koerner, D.W., Meier, R., Hines, D.C., Lowrance, P.J., Terrile, R.J., Thompson, R.I., & Rieke, M. 1999, ApJ, 513, L127

Smith, B.A., & Terrile R.J. 1984, Science, 226, 4681

Smith, B.A., Soderblom, L.A., Banfield, D., Barnet, C., Beebe, R.F., Bazilevskii, A.T., Bollinger, K., Boyce, J.M., Briggs, G.A., & Brahic, A. 1989, Science, 246, 1422

Telesco, C.M., Fisher, R.S., Pia, R.K., Knacke, R.F., Dermott, S.F., Wyatt, M.C., Grogan, K., Holmes, E.K., Ghez, A.M., Prato, L., Hartmann, L.W., & Jayawardhana, R. 2000, ApJ, 530, 329

van der Bliek, N.A., Prusti, T., & Waters, L.B.F.M. 1994, A&A, 285, 229

Wyatt, M.C., Dermott, S.F., Telesco, C.M., Fisher, R.S., Grogan, K., Holmes, E.K., & Piña, R.K. 2000, ApJ, 527, 918

Zuckerman, B., & Becklin, E.E. 1993a, ApJ, 406, L25
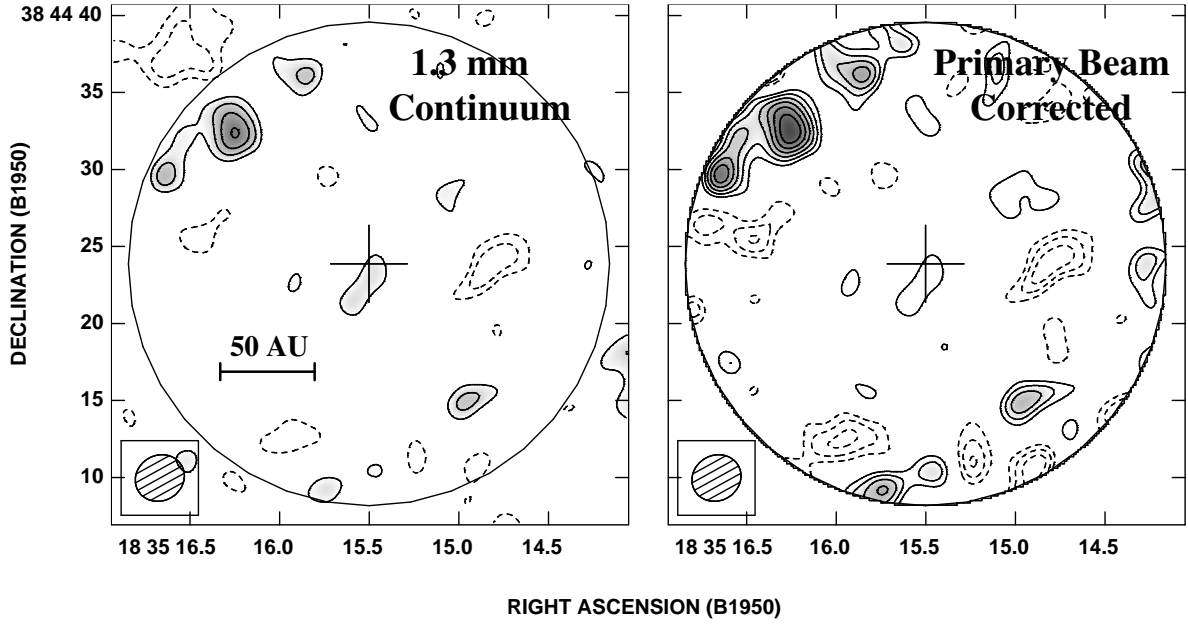
Zuckerman, B., & Becklin, E.E. 1993b, ApJ, 414, 793

Fig. 1.— **Left:** Aperture synthesis image of 1.3 mm emission from Vega (α Lyrae). Contours are at 1σ intervals of 0.5 mJy, starting at the 2σ level. The position of Vega is marked with a cross, the half-power circumference of the primary beam of the 10.4 m telescopes is shown as a circle. The synthesized beam, $3.3'' \times 2.9''$ FWHM at PA 119°, is represented by a hatched circle. **Right:** Same as at left, except that compensation has been made for radial fall-off in intensity due to the primary beam pattern.

Table 1.   Flux Densities in Map

(1) Separation (arc sec)	(2) PA (degrees)	(3) $F_{1.3mm}$ (mJy)	(4) $F_{1.3mm}$ corrected	(5) $F_{0.85mm}$ $\alpha = 2$	(6) $F_{0.85mm}$ $\alpha = 3$	(7) $F_{0.85mm}$ (SCUBA)
12.2±0.6	45	2.5±0.6	4.0±0.9	9.4	14.3	17.3±3
14.5±1.0	67	1.8±0.5	3.4±1.0	8.0	12.2	–
13.0±1.0	18	1.7±0.5	2.8±0.9	6.6	10.0	–
11.0±1.0	215	1.7±0.5	2.4±0.8	5.6	8.6	∼15
0	–	1.4±0.5	1.4±0.5	5±1[a]	5±1	–
Total	–	9.1±1.2	14±1.9	32.9	48.4	45.7±5.4[b]

[a]Represents estimated photospheric flux from Vega at $\lambda = 850\mu$m.

[b]Integrated emission from map of Holland et al. 1998.